International Journal of Nanomedicine

Dovepress
Taylor & Francis Group

Open Access Full Text Article

ORIGINAL RESEARCH

Comparison of the Cytotoxicity, Internalization and Anti-Cancer Drug Delivery Efficacy of Nature Killer Cell Derived Nanovesicles and Extracellular Vesicles

Jing Zhang[1,*], Weili Guan[1,2,*], Ting Guo[3], Yingchun Zhang[1,4], Chulan Gong[5], Rui Ye[1,2], Dan Fang[5], Jinxi Zuo[6], Xiaojin Lin[2,4], Yuting Fan[1,2,7], Zailing Yang[1,2,8], Dan Liang[1,2], Tao Shen[1,2], Liang Chen[9], Xing Zhao[1,2,4]

[1]College of Basic Medical Sciences, Guizhou Medical University, Guiyang, Guizhou, People's Republic of China; [2]Tissue Engineering and Stem Cell Experiment Center, Guizhou Medical University, Guiyang, Guizhou, People's Republic of China; [3]Department of Gynaecology, the Affiliated Hospital of Guizhou Medical University, Guiyang, Guizhou, People's Republic of China; [4]Tumor Immunotherapy Technology Engineering Research Center, Guizhou Medical University, Guiyang, Guizhou, People's Republic of China; [5]Department of Breast Surgery, the Affiliated Hospital of Guizhou Medical University, Guiyang, Guizhou, People's Republic of China; [6]College of Clinical Medicine, Guizhou Medical University, Guiyang, Guizhou, People's Republic of China; [7]Department of Gastroenterology, the Affiliated Hospital of Guizhou Medical University, Guiyang, Guizhou, People's Republic of China; [8]Medical Laboratory, Jinyang Hospital Affiliated to Guizhou Medical University, Guiyang, Guizhou, People's Republic of China; [9]Department of Thoracic and Breast Surgery, Anshun People's Hospital, Anshun, Guizhou, People's Republic of China

*These authors contributed equally to this work

Correspondence: Liang Chen; Xing Zhao, Email 2212521185@qq.com; xingzhao@gmc.edu.cn

Purpose: Natural killer (NK) cell-derived extracellular vesicles (NK-EVs) have garnered significant research interest in the field of tumor immunotherapy. However, the large-scale production of NK-EVs remains a major challenge, limiting their clinical application. This study aims to develop a simple and efficient method for the preparation of NK cell-derived nanovesicles (NK-NVs) and to evaluate their cytotoxicity and drug delivery potential.

Methods: In this study, we efficiently produced large quantities of NK-NVs by extruding NK cells. We conducted comprehensive characterization and protein profiling analyses of NK cells, NK-EVs, and NK-NVs. The cytotoxicity and cellular uptake of NK-NVs were evaluated, and the internalization mechanism was explored. To assess the drug delivery capability, doxorubicin (DOX) was loaded into NK-NVs (NK-NVs-DOX) using various loading strategies, including co-incubation, sonication, extrusion, and electroporation. We thoroughly evaluated the drug loading efficiency, particle size, stability, and cytotoxicity of NK-NVs-DOX.

Results: Extrusion-derived NK-NVs exhibited a remarkable 402.18-fold increase in particle yield and a 325.76-fold enhancement in protein yield compared to ultracentrifugation-isolated NK-EVs, while maintaining comparable morphology and EV-specific markers (Alix, TSG101, CD9). Functionally, NK-NVs induced delayed cytotoxicity against cancer cells via caveolin-mediated endocytosis, selectively sparing normal cells. Proteomic analysis revealed that NK-NVs shared 7,366 proteins with NK cells, surpassing the 5,326 proteins found in NK-EVs. Furthermore, extrusion-optimized NK-NVs-DOX demonstrated pH-sensitive drug release (30% higher at pH 5.5), significantly enhanced anti-cancer effects across four cancer cell lines, and stable drug retention for up to 28 days at 4°C, highlighting their promising therapeutic potential.

Conclusion: Extrusion-derived NK-NVs offer a low-cost, rapid, and high-yield production method while selectively inducing cytotoxicity in cancer cells. Their pH-sensitive drug release enhances drug loading stability. These advantages establish NK-NVs as a promising and scalable platform for tumor immunotherapy and drug delivery with significant clinical potential.

Keywords: natural killer cells, nanovesicles, extracellular vesicles, internalization, drug delivery, antitumor therapy

Received: 12 March 2025
Accepted: 28 August 2025
Published: 2 September 2025

Introduction

Natural killer (NK) cells are cytotoxic lymphocytes capable of directly kill target cells without requiring antigen presentation, playing an important role in cancer cell recognition and eradication.[1] Adoptive NK cell combined with chemotherapy demonstrates significantly growth suppression in cancer cells.[2] However, NK cell immunotherapy is limited by its insufficient cellular infiltration and inadequate proliferative capacity at the tumor site. In addition, cancer cells can develop "escape variants" to cause NK cells to be immunosuppressed in the tumor microenvironment. These mechanisms substantially diminish the tumoricidal efficacy of NK cells during therapeutic intervention.[3]

NK cell derived extracellular vesicles (EVs, NK-EVs) overcomes these shortcomings very well. EVs have emerged as promising therapeutic agents for tumor treatment due to their natural ability to facilitate intercellular communication.[4] These vesicles, secreted by various cell types, carry bioactive molecules such as proteins, lipids, and nucleic acids that can influence the tumor microenvironment and immune responses.[5] Recent advancements in EV-based drug delivery systems have shown their potential to overcome challenges faced by conventional therapies, such as poor bioavailability and rapid clearance.[6] By loading therapeutic agents, including chemotherapeutic drugs, miRNA, or immune modulators, EVs can directly deliver these cargoes to cancer cells, improving treatment efficacy while minimizing off-target effects.[7] NK-EVs carry cytotoxic proteins, such as granzyme, TNF-α and perforin, which can directly diffuse into cancer cells and exert cytotoxicity.[8] Additionally, due to their unique biocompatibility and high penetration capacity, NK-EVs also show significant advantages as drug delivery carriers.[7] Our previous studies found that NK-EVs exhibit cytotoxicity against ovarian cancer (OC) cells, and that NK-EVs loaded with cisplatin can enhance the sensitivity of cisplatin-resistant OC cells to cisplatin.[8] However, the complex and costly processes involved in the preparation and purification of EVs have limited their clinical application, including that of NK-EVs. Therefore, there is an urgent need to develop low-cost, rapid, and high-yield methods for the preparation of NK-EVs to facilitate the clinical translation of NK-EVs.

Recently, researchers have explored various physical and chemical methods to produce large quantities EVs, aiming to improve scalability and efficiency for clinical translation.[1] Through physical methods such as extrusion, ultrasonication, and freeze-thawing, donor cells can release a large number of cell-derived nanovesicles (NVs) in a short time by disrupting the cell membrane using shear or frictional forces, followed by the reorganization of lipid bilayers to form vesicles within seconds.[9] Among these methods, extrusion involves passing cells through filters with varying pore sizes to prepare NVs.[10,11] NVs prepared by extrusion share the same cell membrane as the originating cells, contain the intracellular contents of originating cells, and functions similar to those cells, but the preparation method is simpler and yields higher quantities compared to EVs. NVs derived from mesenchymal stem cells (MSC-NVs) prepared by extrusion exhibit repair-promoting functions, such as enhancing skin regeneration and bone repair, similar to the biological functions of MSC-EVs.[12–14] Zhu et al obtained a total protein yield of NK cell-derived NVs (NK-NVs) that was 13.74 times higher than that of NK-EVs using the same number of cells, displayed more potent cytotoxicity against various cancer cell lines compared with NK-EVs.[15] However, while studies have reported the preparation of NK-NVs via extrusion and highlighted its advantages over NK-EVs production, a comprehensive comparison of their functions and cargo composition has yet to be conducted. Additionally, the mechanism of cellular internalization of NK-NVs and their drug-loading capacity remain unclear.

In this study, we first prepared NK-NVs using the extrusion method and compared them to NK-EVs in terms of yield, characterization, proteomics, and cytotoxicity. Compared to NK-EVs, NK-NVs exhibited a slower killing effect on cancer cells, with noticeable cytotoxicity occurring only after 24 hours. Therefore, we also investigated the mechanism of NK-NVs internalization in cancer cells. Our previous research has reported that NK-EVs are promising carriers for anti-cancer drug delivery.[1] In this study, we further evaluated the ability of NK-NVs to deliver doxorubicin (DOX), and compared the differences between various drug-loading methods in terms of drug loading rate, vesicle particle size, and cytotoxicity against cancer cells. This research lays the theoretical and experimental foundation for future studies on the delivery of anti-cancer drug using NK-NVs.

Materials and Methods

Cell Culture

Human OC cell line SKOV3, COC1/DDP and A2780 were obtained from the China Center for Type Culture Collection; human pancreatic cancer (PC) cell line Panc-1 were obtained from Haixing Biotechnology Co., LTD; human NK92MI cells and human ovarian epithelial cell line IOSE80 were obtained from Procell Life Science&Technology Co., Ltd. SKOV3 cells were cultured in McCoy's 5a medium (Gibco, Gaithersburg, MD, USA); Panc-1 were cultured in Dulbecco's modified eagle's medium (DMEM, Gibco); IOSE80, A2780 and COC1/DDP were cultured in RPMI 1640 medium (Gibco); and human NK92MI cells were cultured in MEMα medium (Gibco). All cultural medium were supplemented with 10% fetal bovine serum (FBS) and 1% penicillin/streptomycin (Gibco). All cells were maintained at 37°C under a humidified atmosphere of 5% CO_2/95% air in an incubator.

Preparation of NK-EVs and NK-NVs

A differential ultracentrifugation method was used for NK-EVs isolation.[14] Briefly, NK cells were cultured in conditioned medium containing 5% exosome-free FBS for 48h and the supernatants was centrifuged at 300 g and 2000 g for 10 min to remove cells and large vesicles. The supernatant was centrifuged at 10, 000 g for 30 min and centrifugation at 10, 0000 g for 70 min twice, then the NK-EVs pellet was resuspended in PBS and filtered through a 0.22 μm filter.

A serial extrusion method was used for NK-NVs production. NK cells were collected and rinsed twice with PBS buffer before cell counting. 2×10^6 cells/mL were resuspended using 1 mL PBS and subjected to sonication for fragmentation, then the supernatants were centrifuged for 10 min at 500 g. Next, the supernatants were extruded using a Liposome extruder (Avanti Polar Lipids, Inc., USA) through a set of polycarbonate membranes with nanopore sizes (10, 5, and 1 μm, Whatman) sequentially. Following that, the extruded liquid was centrifuged at 10,000 g for 30 minutes. The supernatant was collected and then filtered through a 0.22 μm filter. The obtained NK-EVs and NK-NVs were stored at −80°C for use in subsequent experiments.

Characterization of NK-NVs

The obtained NK-EVs and NK-NVs was observed by transmission electron microscope (TEM) for morphological characterization. The samples were mounted onto the copper grid for 5 min, and excess liquid removed with filter paper. 2% phosphotungstate acid was loaded onto the copper grid for 1~2 min at room temperature, and excess liquid was removed with filter paper. After air dying the samples, the images were observed and recorded by TEM instrument (HT-770, Hitachi, Japan).

The particle size distribution and concentration were measured by Nanocoulter counter (Resuntech, Co., Ltd, Shenzhen, China). The samples were adjusted to the appropriate concentration before testing. The total protein concentration was measured with BCA protein assay (Beyotime, China) following the manufacturer's instructions.

The presence of key marker was examined by western blot, primary antibodies used above include anti-CD9 (HY-P80610, MCE), anti-TSG101 (HY-P80924, MCE), anti-Alix (HY-P80011, MCE), anti-Calnexin (Biodragon), anti-CD56 (CST), anti-perforin (Biodragon), anti-granzyme B (Biodragon) and secondary antibodies HRP-labelled goat anti-rabbit IgG (Servicebio, GB23303) to detect relative expression of target proteins. The images were visualized by chemiluminescence (Bio-Rad Laboratories, USA).

Profiling of Total Proteins with Mass Spectrometry

Take out all the samples (NK cells, NK-EVs and NK-NVs) in the frozen state and add an appropriate amount of protein lysis buffer. Use a high-throughput tissue grinder to oscillate the samples three times. Perform non-contact low-temperature ultrasonication for 30 min. Centrifuge at 14,000 g for 15 min and collect the supernatant. Subsequently, protein concentration of NK cells, NK-EVs and NK-NVs was measured by BCA protein assay. Protein samples (100 μg) were lysed, supplemented with 100 mM TEAB, reduced with 10 mM TCEP (37°C, 60 min), and alkylated with 40 mM IAA (dark, RT, 40 min). Proteins were precipitated using acetone (6:1 v/v, −20°C, 4 h), centrifuged (10,000 g, 20 min), resuspended in 100 μL 100 mM TEAB, and digested with trypsin (1:50 w/w, 37°C, overnight). Peptides were dried,

reconstituted in 0.1% TFA, desalted, concentrated, and quantified via UV spectrophotometry (NANO DROP ONE, Thermo Scientific). For DIA mass spectrometry, peptides were separated using Vanquish Neo UHPLC (Thermo Fisher) with an 8-min gradient and analyzed on an Orbitrap Astral mass spectrometer (DIA mode, 100–1700 m/z, 1.5 kV ion source). Data were processed with Spectronaut v19 (peptide length 7–52, trypsin/P cleavage, max 2 missed cleavages, fixed carbamidomethylation, variable methionine oxidation/N-terminal acetylation, FDR ≤ 0.01%). Protein quantification was performed using MaxLFQ. Bioinformatics analysis, including gene ontology (GO) /KEGG functional annotation and STRING protein interaction analysis, was conducted via Majorbio Cloud.

Preparation of NK-NVs-DOX

DOX (Shenzhen Wanle Pharmaceutical Co., Ltd.) was diluted to a concentration of 10 mM using 0.9% saline for subsequent experiments. The absorbance of the DOX solutions at 480 nm was measured using the microplate reader (Synergy H1, BioTek Instruments), and a standard curve was then constructed based on the measured absorbance data. The concentration of DOX in subsequent experiments was determined by referring to the standard curve.

The protein concentration of NK-NVs was normalized to 100 μg/mL, and DOX was added to NK-NVs at different concentrations in the corresponding experiments. The DOX was loaded into the NK-NVs using four different methods: co-incubation: incubating the mixture at 37°C for 1 hour; electroporation: applying pulses at 450 V for 120 ms by Celetrix electroporation system (Celetrix, Manassas, VA, USA); extrusion: extruding the mixture 20 times through a 200 nm polycarbonate membrane by a liposome extruder; sonication: conducting a 30% amplitude, 20s on/off cycle by ultrasonic disruptor (BioSafer 650–92, China). After loading, the mixture was centrifuged at 100,000 g for 70 minutes to collect the supernatant (which contains free DOX). The pellet was resuspended in 50 μL PBS for further experimental analysis. The recovery yield of NK-NVs-DOX was to be calculated by dividing the number of recovered NK-NVs-DOX by the number of spiked NK-NVs. The absorbance of the supernatant was measured at a wavelength of 480 nm using a microplate reader to calculate the unencapsulated DOX concentration. The drug-loading efficiency was then calculated using the following formula:

Drug loading % = (amount of total loaded DOX - amount of unloaded DOX) / total NK-NVs weight × 100%

Cell Viability Assays

To assess the cytotoxicity of NK-NVs, SKOV3, COC1/DDP, A2780, Panc-1, and ISOE80 cells were seeded (2×10^4 cells/well) in 96-well plates and cultured overnight. Different concentrations of NK-NVs or NK-EVs (10–100 μg/mL) were added to cancer cells and co-cultured for 24 or 48h at 37°C. To evaluate the cytotoxicity of NK-NV-DOX prepared by different loading strategies against cancer cells, SKOV3, COC1/DDP, A2780 and Panc-1 cells were seeded at 2×10^4 cells per well in 96-well plates and cultured overnight to ensure complete adherence. Equal amounts of NK-NVs (10 μg/mL), DOX and NK-NVs-DOX (1.5 μg/mL) were added to cancer cells and co-cultured at 37°C for 24h. 10 μL of detection reagents from Cell Counting Kit-8 (CCK-8; meilunbio, China) were added to cultured cells and incubated at 37°C for 2h before optical densities (ODs) were measured at 450 nm. Measurements were performed in triplicate for each experiment, and all experiments were repeated three times. Cell viability was calculated by the following formula:

Cell viability % = $(OD_{experiment} - OD_{blank}) / (OD_{control} - OD_{blank}) \times 100\%$

Internalization of NK-NVs

For the internalization of NK-NVs assays, NK-NVs were labeled with DiO (MCE, HY-D0969) and free dye was removed using centrifugation with a 100 kDa ultrafiltration tube. Panc-1 and SKOV3 cells were co-cultured with DiO-labeled NK-NVs for 3, 6, 12, 24h, respectively. Then the cells were washed in PBS and fixed in 4% paraformaldehyde, and the cell nuclei were stained with 10 μg/mL DAPI. To further explore the mechanism of NK-NVs internalization by cancer cells, three endocytosis inhibitors were employed: 10 μM Chlorpromazine (CPZ), 10 μM methyl-β-cyclodextrin (MβCD), and 1 μM wortmannin, purchased from Shandong Topscience Biotech Co. Ltd. Cancer cells were pretreated with the inhibitors for 2h before being subjected to the same experimental procedure as described above. All the images were acquired by laser scanning confocal microscope (Nikon, AX) and the fluorescence intensity of intracellular DiO-labeled NK-NVs was analyzed using Image J 1.53e software.

Release Profile of NK-NVs-DOX

For *in-vitro* drug release studies, 100 μg NK-NVs-DOX was dispersed in a dialysis bag (molecular weight cut off of 12,000~14,000) containing 1 mL PBS. The dialysis bags were immersed in 50 mL Eppendorf tubes containing 20 mL PBS at pH 5.5 and 7.4, respectively. The tubes were placed on a rotating shaker inside a 37°C incubator and rotated at 70 rpm under light-protected conditions. Sampling of the release PBS was carried out at different time intervals (0, 0.5, 1, 2, 3, 6, 12, 24, 48h) and replaced with an equal volume of PBS to maintain constant conditions. The experiments were conducted in triplicate. The DOX released was quantified by microplate reader as described above.

Flow Cytometry

COC1/DDP cells were pretreated with NK-NVs for 24h and cell apoptosis was evaluated by flow cytometry analysis using Annexin V-AF647/PI apoptosis kit (Goonie, China). Cells were washed in precooled PBS twice and suspended in 1× binding buffer, incubated in the dark with Annexin V-AF647 and PI for 15 min, then add 1 × Binding Buffer and mix gently before analyzed by flow cytometry (BD LSR Fortessa 4, USA), and the data were analyzed using FlowJo 10 software.

Statistical Analyses

All experiments were repeated at least three times. All statistical analyses were performed using GraphPad Prism 8.0.2, and the data are expressed as the mean± SEM. P value< 0.05 was considered statistically significant by using the Student's t-test: *p< 0.05, **p<0.01 and ***p< 0.001.

Results

Comparison of Yield, Morphology, and Stability Between NK-NVs and NK-EVs

The preparation process of NK-NVs is illustrated in Figure 1A, with the yield of NK-NVs obtained by extrusion was evaluated. After extruded, 10^{10} NK cells produced approximately $4.11\times10^{14} \pm 5.09\times10^{12}$ particles with a total protein content of 1616.73 ± 31.75 mg. Compared to NK-EVs isolated by ultracentrifugation from the supernatants, this method resulted in about a 402.18-fold increase in particle yield and a 325.76-fold increase in protein yield (Figure 1B and C).

Subsequently, the morphological characteristics of NK-NVs was analyzed. TEM imaging revealed a lipid bilayer membrane structure and spherical morphology of NK-NVs (Figure 1D), which are similar to NK-EVs. The average particle size of NK-NVs detected by Nanocoulter counter is about 78 ± 29.8 nm (Figure 1E). Western blot analysis of NK-NVs preparations confirmed the presence of EV-specific markers Alix, TSG101 and CD9, while the negative marker calnexin was detected only in NK cell lysates (Figure 1F). To evaluate the storage stability, the particle size of NK-NVs stored at 4°C or −80°C was monitored from day 1 (preparation day) to day 28. As shown in Figure S1A and B, the particle size of NK-NVs stored at 4°C exhibited an increasing trend after 5 days, whereas it remained relatively constant during the first 5 days or under −80°C storage condition.

Therefore, both NK-NVs and NK-EVs exhibited similar particle sizes, morphology, and protein markers. However, the yield of NK-NVs was notably higher, and its particle size remained stable when stored at −80°C, highlighting the efficiency of our protocol in producing NVs with comparable characteristics.

Comparison of Cytotoxicity of NK-NVs and NK-EVs Against Different Cancer Cells in vitro

NK cells are known to exert their cytolytic activity through the release of cytotoxic effectors (ie, granzyme B and perforin) contained in lytic granules. Upon target cell recognition and conjugation, the granules are actively directed to the site of cell−cell contact, and soluble effector molecules are released into the forming cytotoxic immunological synapse.[16] Thus, we first demonstrated the presence of CD56 (marker of NK cell) in NK-NVs by western blot, and subsequently revealed the presence of both granzyme B and perforin in NK-NVs (Figure 2A).

Whereas NK-NVs and NK-EVs internalized by cancer cells via endocytosis to deliver cytotoxic substances, NK cells necessitate surface receptor-mediated membrane contact to trigger cytotoxic substances. Therefore, we focused on

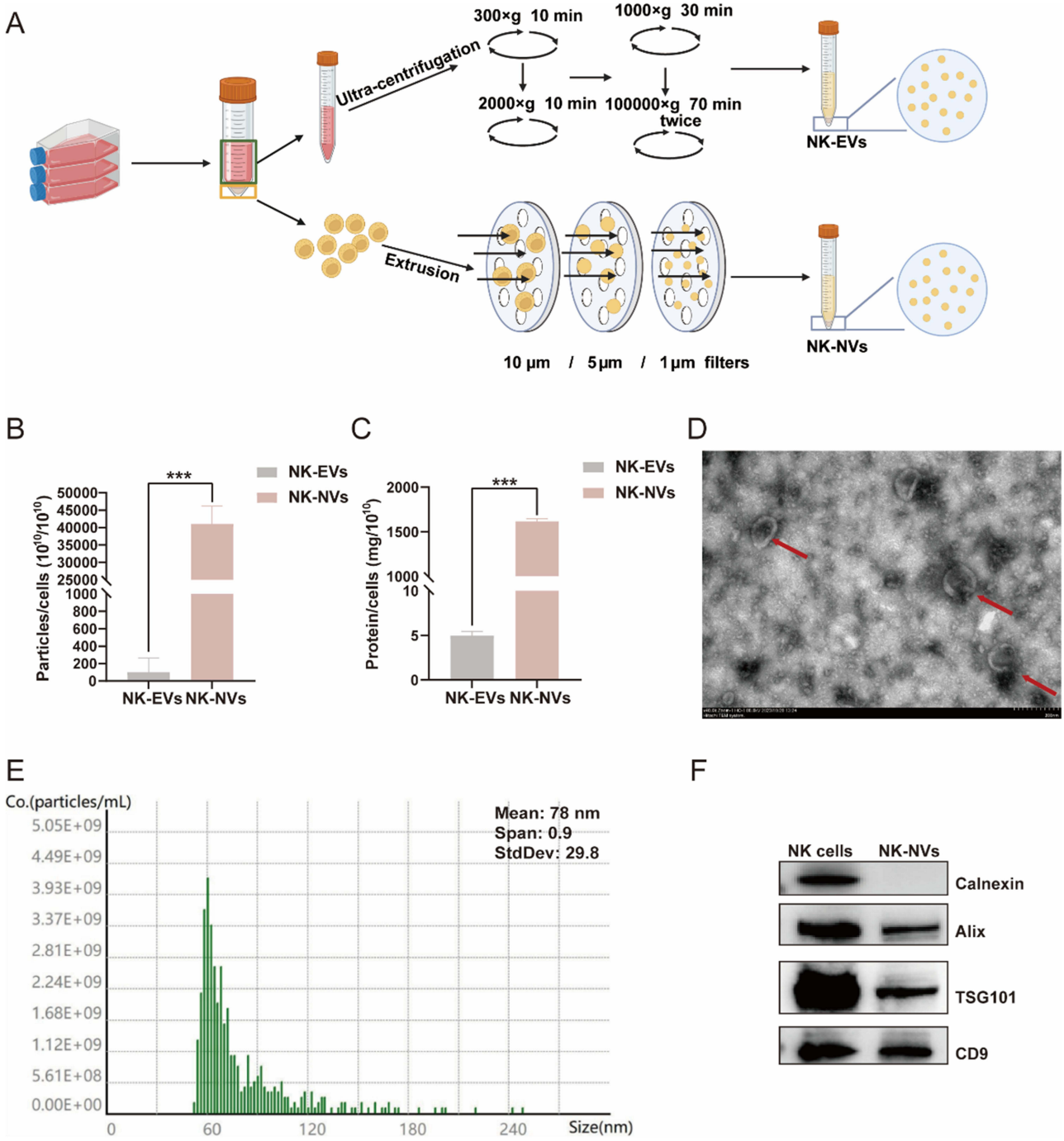

Figure 1 Comparison of morphology characterization and yield of NK-EVs and NK-NVs. (**A**) Schematic illustration of the generation process of NK-EVs and NK-NVs. (**B**) The yields of NK-EVs and NK-NVs measured as the particle. (**C**) The yields of NK-EVs and NK-NVs measured as the total protein. (**D**) TEM images showing the particle size, structure and spherical morphology of NK-NVs. (**E**) Size distribution of NK-NVs indicated by Nanocoulter counter. (**F**) Western blot analysis of exosomal and NK cell marker proteins on NK-NVs. Data are present as the mean ± SD of three independent biological samples. *** $p<0.001$.

comparing the cytotoxic effects of NK-NVs and NK-EVs on cancer cells. Both NK-NVs and NK-EVs exhibited dose-dependent cytotoxicity against the three OC cell lines, COC1/DDP, SKOV3, and A2780. However, the PC cell line Panc-1 was not sensitive to the cytotoxic effects of either NK-NVs or NK-EVs (Figure 2B). Overall, at the 24-hour time point, NK-NVs showed lower cytotoxicity against cancer cells compared to NK-EVs. However, when the incubation time with NK-NVs was extended to 48 hours, a significant increase in cytotoxicity against cancer cells was observed, suggesting that the cytotoxic effect of NK-NVs is delayed compared to that of NK-EVs (Figure 2C). In addition, to evaluate the

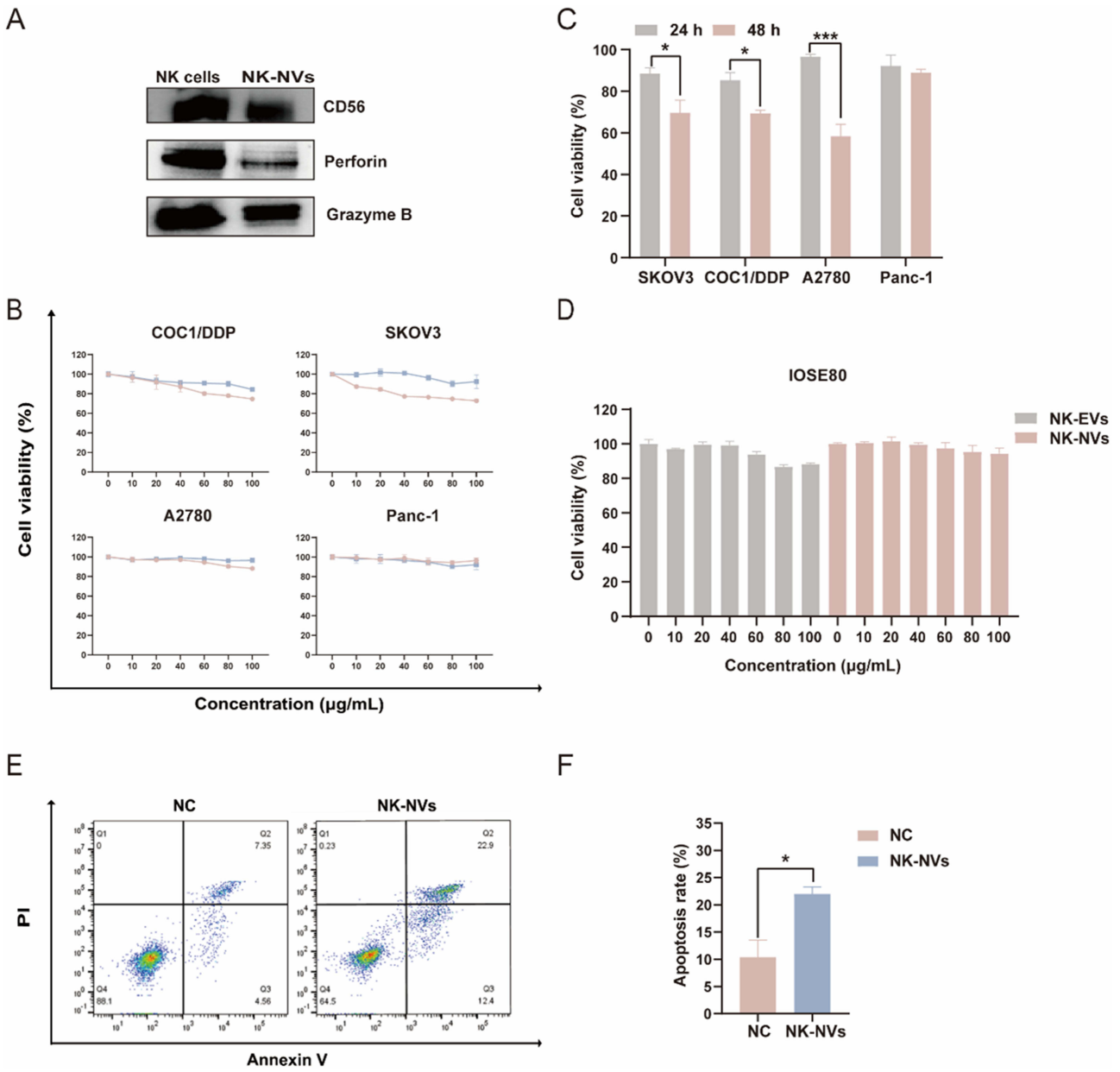

Figure 2 Comparison of cytotoxicity of NK-NVs and NK-EVs against different cancer cells in vitro.(**A**) Western blot analysis of perforin and granzyme expression in NK cells and NK-NVs. (**B**) The cell viability of cancer cells after 24h co-incubation with NK-NVs and NK-EVs by CCK-8 assay (blue: NK-NVs, red: NK-EVs). (**C**) The cell viability of cancer cells after co-incubation with NK-NVs for 24 and 48h by CCK-8 assay. (**D**) The cell viability of IOSE80 cells after 24h co-incubation with NK-NVs and NK-EVs by CCK-8 assay. (**E** and **F**) Flow cytometry was performed to analyze the apoptosis rate of COC1/DDP cells (Annexin V/PI double staining, NC: negative control). Data are present as the mean ± SD of three independent biological samples. * $p<0.05$, *** $p<0.001$.

effects of NK-NVs on normal cells, we investigated the effects of both NK-NVs and NK-EVs on IOSE80 cell activity (Figure 2D). Similar to NK-EVs, we observed that NK-NVs had no significant effect on IOSE80 viability at the highest concentration of 100 μg/mL. These results suggest that NK-NVs specifically kill cancer cells and are safe for normal cells. This specific killing of cancer cells by NK-NVs is also similar to that of NK cells and NK-EVs, and the mechanisms involved need to be further investigated.

Inducing apoptosis in target cells through the release of cytotoxic substances is the primary mechanism by which NK cells kill cancer cells.[17] We next investigated whether NK-NVs could induce apoptosis in cancer cells in a similar manner to NK cells. Flow cytometry was performed to analyze the apoptosis of COC1/DDP cells after treatment with NK-NVs for 24 hours. As shown in Figure 2E and F, the proportions of apoptotic cells, including both late apoptotic (Annexin V^+/

https://doi.org/10.2147/IJN.S527756

PI^+) and early apoptotic cells (Annexin V^+/PI^-), were significantly higher in NK-NVs treated cells compared to untreated cells (22% ± 1.27% vs 10.41% ± 3.10%).

Identification of the Differentially Expressed Proteins

To investigate the differences in protein composition, we analyzed the expression patterns of the entire protein profile across NK cells, NK-NVs, and NK-EVs using proteomics. This comparison revealed distinct variations in the protein profiles, providing insights into the unique molecular characteristics of each sample. We identified 7504, 7459 and 5358 proteins from NK cells, NK-NVs and NK-EVs, respectively. A total of 7,366 mutual proteins were found between NK-NVs and NK cells, while only 5,326 were found between NK-EVs and NK cells (Figure 3A). Therefore, NK-NVs and NK cells showed a more similar protein profiling.

We further performed GO analysis of NK-EVs and NK-NVs proteins and annotated their biological process, molecular function and sub-cellular location (Figure 3B). The predominant proteins identified in NK-NVs and NK-EVs are primarily involved in nucleic acid metabolism, metabolism regulation, and protein interaction networks, indicating that the molecular functions of NK-NVs and NK-EVs are similar to a certain extend. The predominant proteins in NK-NVs and NK-EVs are found in organelles and cell membranes, with NK-NVs having more of these proteins from NK cells. This may be due to the fact that a large number of cytoplasmic or membranal proteins can be encapsulated into NK-NVs during extrusion. KEGG enrichment analysis of NK-NVs and NK-EVs proteins showed that, compared to NK-EVs, the up-regulated proteins in NK-NVs are primarily enriched in metabolic pathways. In contrast, the downregulated proteins are mainly enriched in proteins involved in immune responses against human diseases such as malaria infection, complement and coagulation cascades (Figure 3C and D).

Our previous research has shown that NK-NVs possess cancer cell-killing function. However, compared to NK-EVs, their cytotoxic effect occurs with a relative delay. This suggests that the process of NK-NVs entering cancer cells or the contents within NK-NVs that may induce cytotoxicity are involved. Therefore, we further analyzed the differences in the expression of proteins associated with endocytosis and NK cells mediated cell death pathways. Among proteins involved in the endocytosis pathway, the expression of F-actin-capping protein and actin-related protein in NK-NVs was higher than in NK-EVs, suggesting that there are many cytoskeletal proteins in NK-NVs (Figure 3E). Among proteins involved in the NK cells mediated cell death pathway, all of NK cells, NK-NVs and NK-EVs have similar protein expression profile, but NK-EVs show significantly higher expression of granzyme B (Figure 3F). It is particularly noteworthy that the expression of BiP, an endoplasmic reticulum (ER) chaperone and master regulator of ER functions, is significantly higher in NK-NVs than in NK-EVs. Previous studies have demonstrated that NK-EVs induce cell death in target cells via ER stress.[18] The elevated expression of BiP in NK-NVs suggests a potential link between BiP and their cytotoxicity. ER stress may also play a crucial role in this process, potentially contributing to the delayed cytotoxic effect observed with NK-NVs.

NK-NVs are Internalized by Cancer Cells via Caveolin-Mediated Endocytosis Pathway

As observed earlier, NK-NVs exhibit a delayed cytotoxic effect on cancer cells compared to NK-EVs. We hypothesized that this delay may be related to differences in the mechanisms by which NK-NVs exert their tumor-killing effects or the delay in their uptake by cancer cells. Therefore, we first dynamically observed the uptake of NK-NVs by cancer cells using confocal laser microscopy. As shown in Figure 4A–D, NK-NVs (labeled with DiO dye, green) began to accumulate in Panc-1 and SKOV3 cells (nuclei labeled with DAPI dye, blue) at 3h, with the accumulation gradually increasing over time. After 24h, substantial uptake of NK-NVs by both Panc-1 and SKOV3 cancer cells was observed. According to previous studies, the internalization of NK-EVs occurs much earlier than that of NK-NVs, with NK-EVs being detectable intracellularly within 30 minutes to 1h, reaching a plateau at 14h.[19] As a result, NK-EVs can achieve maximal cytotoxicity at 24h. This explains why, in our study, NK-NVs exhibited a delayed cytotoxic effect compared to NK-EVs.

There may be multiple endocytic routes involved in the internalization of NK-NVs by cancer cells. To further investigate the routes associated with NK-NVs internalization, we pretreated SKOV3 and Panc-1 cells with three different inhibitors targeting specific endocytic pathways. These included CPZ to inhibit the clathrin-mediated endocytic pathway, MβCD to block the caveolin-mediated endocytic pathway, and wortmannin, a specific PI3K inhibitor, to inhibit

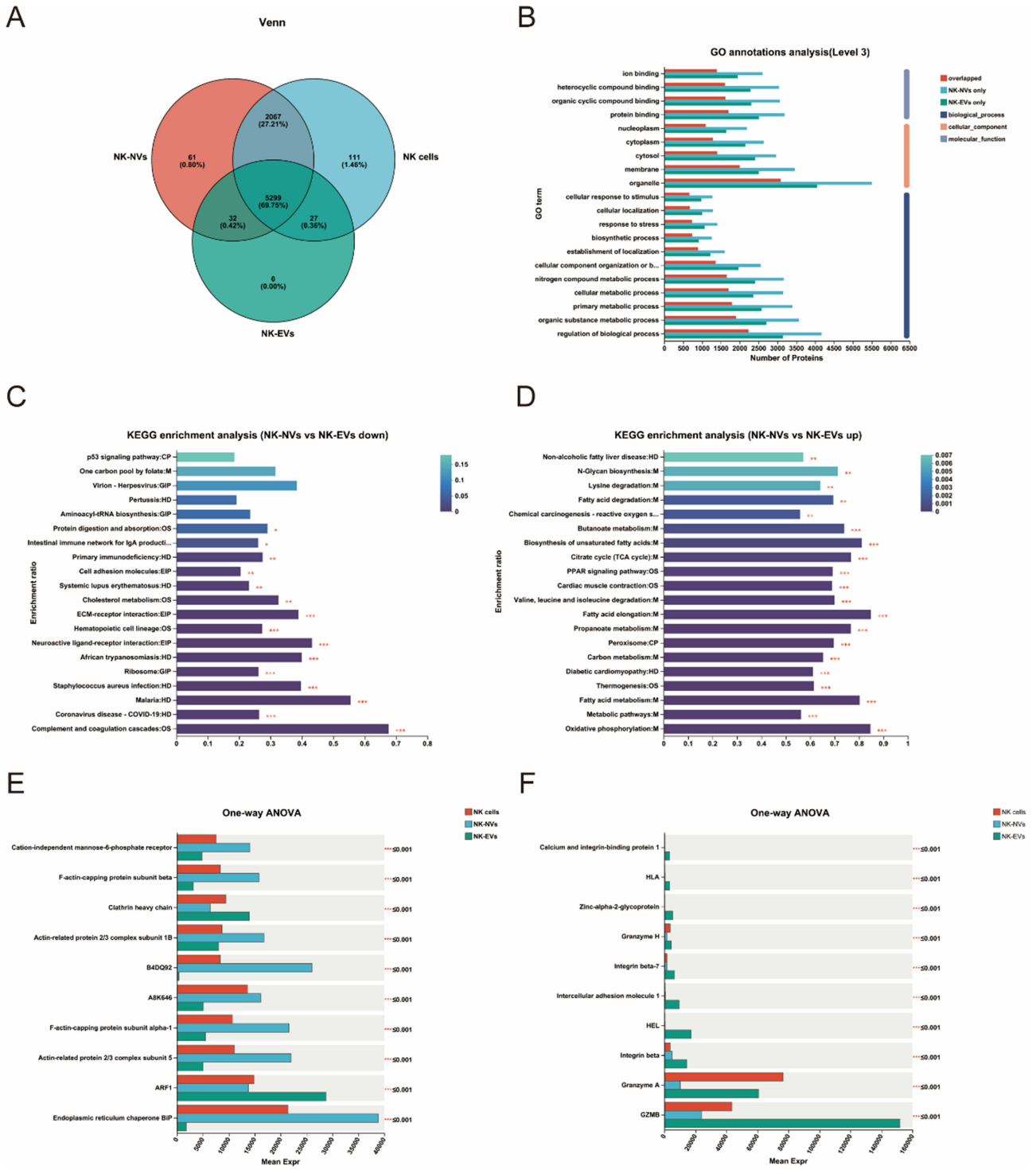

Figure 3 Identification of the differentially expressed proteins among NK cells, NK-EVs and NK-NVs. (**A**) Venn diagram depicting the overlap of proteins, which were identified from the 3 biological replicates of NK cells, NK-EVs and NK-NVs. (**B**) GO annotations analysis of differentially expressed proteins for NK-EVs and NK-NVs. (**C** and **D**) KEGG enrichment analysis of differentially expressed proteins for NK-EVs and NK-NVs. *P*-values and fold change for proteins between two groups were calculated using the R package "Welch's Test" and **p*<0.05 ***p*<0.01, ****p*<0.001. (**E**) Comparison of the number of unique proteins detected in NK cells, NK-EVs and NK-NVs that are associated with the endocytosis pathway. *P*-values as determined by one-way ANOVA, and **p*<0.05 ***p*<0.01, ****p*<0.001. (**F**) Comparison of the number of unique proteins detected in NK cells, NK-EVs and NK-NVs that are associated with the NK cells mediated cell death pathway. *P*-values as determined by one-way ANOVA, and **p*<0.05 ***p*<0.01, ****p*<0.001.

https://doi.org/10.2147/IJN.S527756

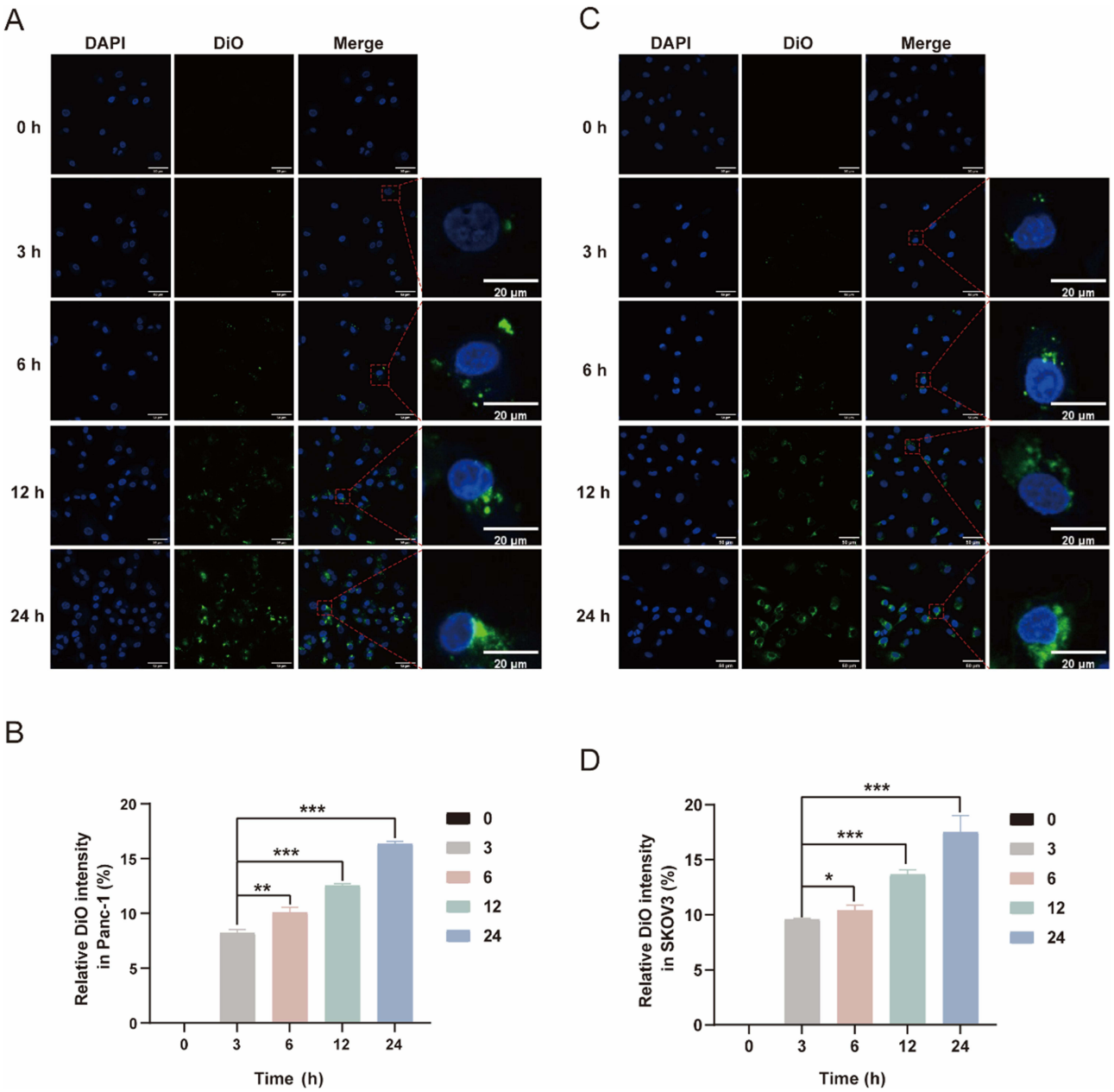

Figure 4 Internalization of NK-NVs by cancer cells. (**A** and **B**) Confocal microscopy analysis of Panc-1 cells after co-incubation with DiO-labelled NK-NVs at different time periods (3, 6, 12 and 24h). (**C** and **D**) Confocal microscopy analysis of SKOV3 cells after co-incubation with DiO-labelled NK-NVs at different time periods (3, 6, 12 and 24h). Data are present as the mean ± SD of three independent biological samples. *p<0.05 **p<0.01, ***p<0.001.

macropinocytosis-mediated endocytosis. After two hours of pretreatment, confocal microscopy images revealed that the internalization of NK-NVs was significantly inhibited following MβCD pretreatment, while CPZ and wortmannin inhibitors had minimal effects (Figure 5A–D). Further analysis showed that the cytotoxicity of NK-NVs against SKOV3 and Panc-1 cells was also inhibited after pretreatment with MβCD (Figure 5E). These results suggest that NK-NVs may enter cancer cells via the caveolin-mediated endocytic pathway.

Evaluation of Four Loading Strategies for NK-NVs-DOX and Their Cytotoxic Effects

As cell-derived nanoscale vesicles similar to EVs, NK-NVs exhibit excellent biocompatibility and can accumulate at tumor sites due to the enhanced permeability and retention (EPR) effect. This makes them an effective tool for anti-cancer drug delivery in cancer therapy. Therefore, we further evaluated the drug delivery capabilities of NK-NVs. In this

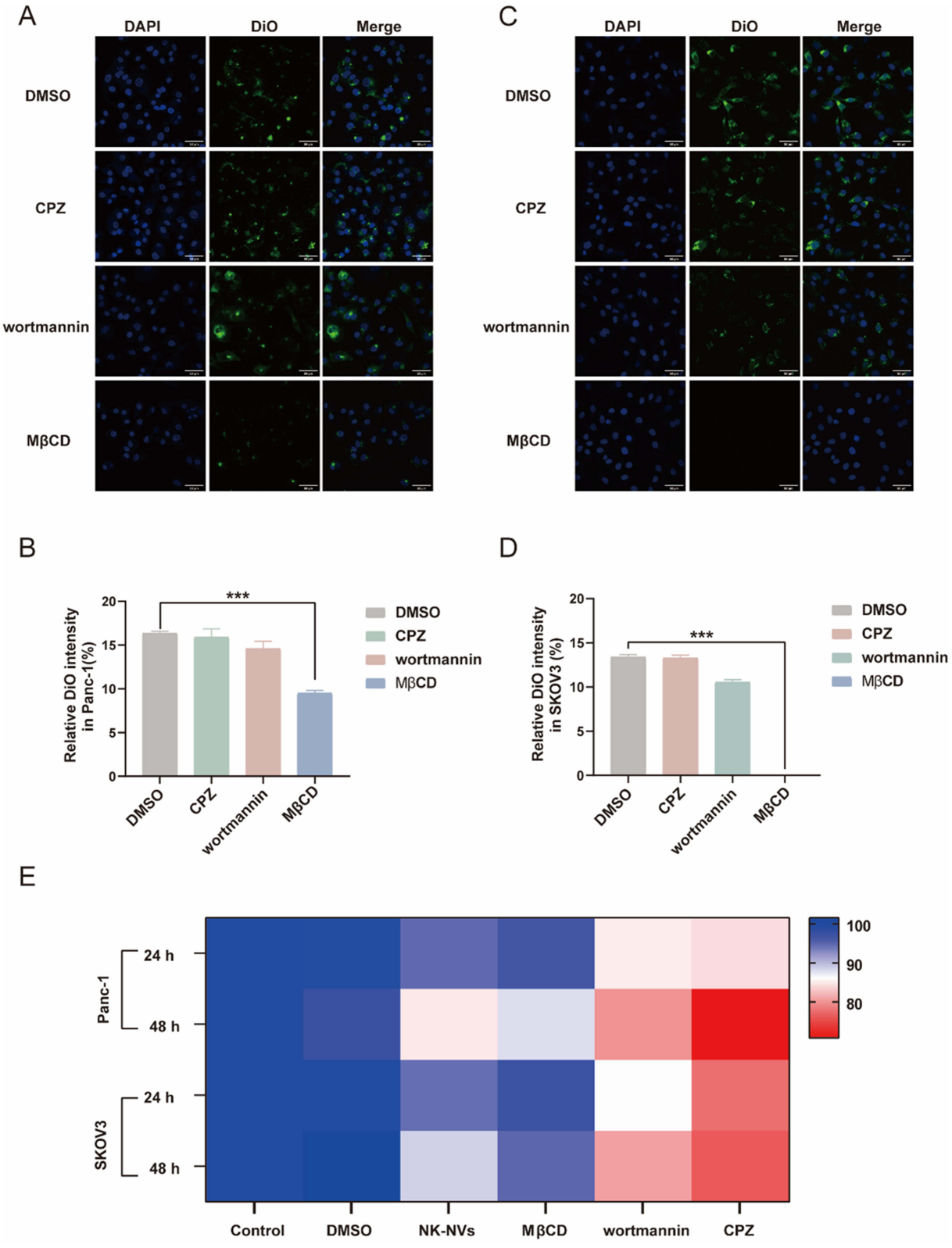

Figure 5 Internalization mechanisms of NK-NVs by cancer cells. (**A** and **B**) Confocal microscopy analysis of endocytosis inhibitor pretreated Panc-1 cells after co-incubation with DiO-labelled NK-NVs at 24h. (**C** and **D**) Confocal microscopy analysis of different endocytosis inhibitor pretreated SKOV3 cells after co-incubation with DiO-labelled NK-NVs at 24h. (**E**) The cell viability of different endocytosis inhibitor pretreated Panc-1 and SKOV3 cells after 24h/48h co-incubation with NK-NVs by CCK-8 assay. Data are present as the mean ± SD of three independent biological samples. ***$p<0.001$.

https://doi.org/10.2147/IJN.S527756

study, DOX, a commonly used broad-spectrum chemotherapeutic agent, was selected to be loaded into NK-NVs to evaluate their drug delivery capabilities. Four different drug loading strategies were compared, including co-incubation, electroporation, extrusion, and sonication (Figure 6A).

Anticancer drugs can be loaded into NVs using various physical or chemical methods. Drug-loaded NVs typically show an increase in particle size, with EVs loss primarily resulting from physical disruption.[20] Sonication, for example, uses mechanical shear forces to damage NVs membranes, causing irreversible aggregation or fragmentation. Extrusion applies repeated mechanical stress, altering membrane integrity and surface properties. Electroporation creates transient pores, destabilizing the membrane and potentially leading to NVs rupture or fusion, thus reducing recoverable yield.[3] Therefore, balancing loading efficiency with the preservation of NVs integrity is crucial. We aimed to balance maximum drug loading and recovery yield with minimal particle size. The average size, recovery yield, and drug loading efficiency of NK-NVs-DOX prepared by different methods were evaluated. Electroporation and extrusion methods achieved the highest drug loading efficiencies (47.37 ± 1.61% and 37.68 ± 4.42%, respectively), while the co-incubation method yielded the lowest efficiency (18.60 ± 4.71%) (Figure 6B). Particle sizes of NK-NVs-DOX, measured using a Nanocoulter counter with nanopore chips (60~200 nm range), showed minimal variation across methods, all remaining under 100 nm. Extrusion resulted in the highest recovery yield, while electroporation achieved the lowest (Figure 6C). Considering drug loading efficiency, particle size, and recovery rate, extrusion emerged as the optimal preparation method.

We next examined the effect of DOX concentration on the drug loading efficiency in NK-NVs-DOX. As shown in Figure 6D, drug loading peaked at 5 μg/mL DOX before decreasing. The particle size remained consistently below 100 nm, unaffected by DOX concentration. In terms of in vitro cytotoxicity, NK-NVs-DOX prepared by different methods exhibited varying effects. As shown in Figure 6E, NK-NVs-DOX exhibited enhanced cytotoxicity compared to NK-NVs or DOX alone across all four cancer cell lines, with extrusion and electroporation demonstrating the most significant effects. However, considering that the recovery yield of NK-NVs-DOX prepared by electroporation was relatively low, extrusion emerged as the optimal preparation method when taking into account drug loading efficiency, particle size, recovery rate, and cytotoxicity against cancer cells.

Next, we evaluated the stability of NK-NVs-DOX prepared by the extrusion method. As shown in Figure 6F, NK-NVs-DOX demonstrated no significant change in drug loading efficiency over 28 days when stored at 4°C or −80°C. We also assessed the release profile of NK-NVs-DOX at pH 5.5 and pH 7.4 under 37°C for 48 hours. As shown in Figure 6G, an initial burst release occurred within 0.5 hours in both buffer solutions, with significantly higher release at pH 5.5 compared to pH 7.4. Over time, the release gradually increased, reaching saturation at 12 hours. At this point, the release at pH 5.5 was approximately 30% higher than at pH 7.4.

Discussion

NK cells have shown significant promise in tumor therapy, however, challenges such as limited tumor site targeting and immunosuppression of the tumor microenvironment, hinder their clinical application.[21,22] NK-EVs retain key functional properties of NK cells, delivering cytotoxic proteins and immune-regulatory molecules to target cells, thereby enhancing their therapeutic potential. They offer notable advantages, including reduced immunogenicity, enhanced stability, and the ability to carry cytotoxic molecules and therapeutic drugs, enabling targeted delivery and improving both safety and efficacy.[9] However, the preparation of NK-EVs and the efficient loading of therapeutic drugs face challenges such as low yield, heterogeneity, and complex production methods. To address these issues, this study explores large-scale NK-NVs production via extrusion and compares it with conventional NK-EV preparation methods.

In this study, NK-NVs prepared via extrusion through a set of nanopore-sized polycarbonate membranes were found to have similar physicochemical properties, including size, morphology, NK cell and EVs markers, consistent with previous studies.[15,23] The number of particles and protein yield of NK-NVs produced by extrusion were 402.18 times and 325.76 times greater, respectively, than those of NK-EVs produced by the same number of cells, surpassing the yields reported in previous studies.[24] In addition to the higher yield, our method offers advantages in terms of time and labor efficiency, as the extrusion process can be completed within half an hour, whereas the ultracentrifugation method for NK-EVs preparation takes at least 3 hours.

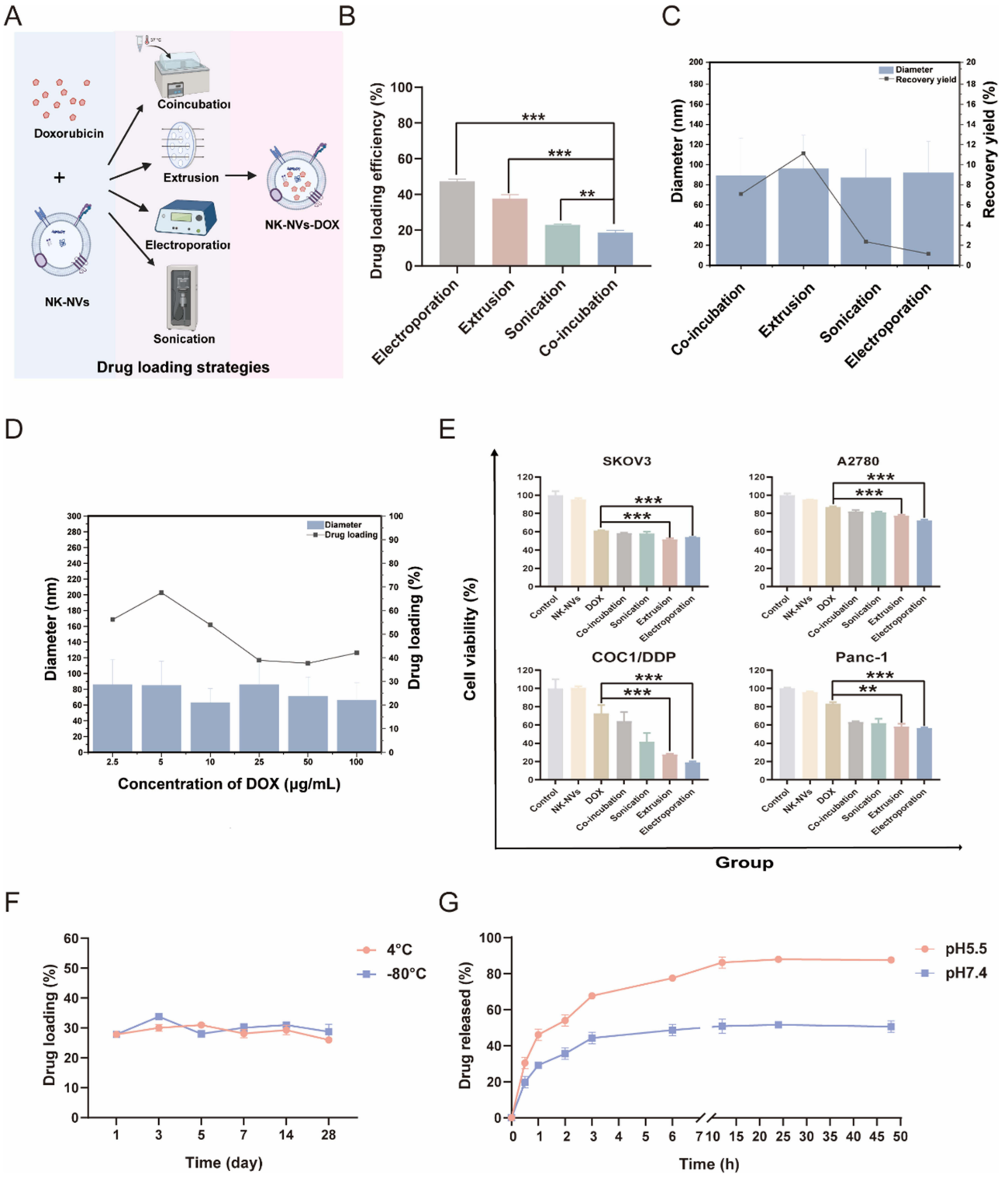

Figure 6 Evaluation of four loading strategies for NK-NVs-DOX and their cytotoxicity. (**A**) Schematic illustration of four loading strategies. (**B**) The drug loading efficiency of DOX for four loading strategies. (**C**) Particle size and recovery yield of NK-NVs-DOX prepared by four loading strategies. (**D**) Particle size and drug loading efficiency of NK-NVs-DOX at different DOX concentrations prepared by extrusion. (**E**) The cell viability of cancer cells after 24h co-incubation with NK-NVs-DOX by CCK-8 assay. (**F**) The drug loading efficiency of NK-NVs-DOX prepared by extrusion stored at 4°C and −80°C. (**G**) The drug release test of NK-NVs-DOX depending on the time and pH conditions at 37°C. Data are present as the mean ± SD of three independent biological samples. ** p<0.01, ***p<0.001.

https://doi.org/10.2147/IJN.S527756

Regarding the cytotoxicity of NK-NVs, killing of multiple cancer cell lines revealed a delayed effect compared to NK-EVs. At the 24-hour time point, NK-NVs showed lower cytotoxicity against cancer cells. However, when the incubation time of NK-NVs with cancer cells was extended to 48 hours, a significant increase in cytotoxicity was observed. We and other studies have demonstrated that NK-EVs can release cytotoxic substances, such as perforin and granzymes, to kill cancer cells.[12,25] Therefore, the slower cytotoxicity of NK-NVs is likely attributed to differences in molecular cargos of NK-NVs and/or the mechanism by which NK-NVs enter cancer cells. In addition, the human PC cell line Panc-1 was insensitive to both NK-NVs and NK-EVs. Even when the co-incubation time was extended to 48 hours, the cytotoxicity of NK-NVs on Panc-1 was significantly lower than that of other cancer cells, such as human OC cell lines SKOV3, A2780 and COC1/DDP. It has been found that differences in protein expression in cancer cells derived from different origins lead to different cytotoxicity of NK cells against target cells.[26–28] Therefore, we supposed that the low sensitivity of Panc-1 to NK-NVs may be related to its intrinsic genetic background, and the specific mechanism will be further explored in future studies.

Proteomic analysis indicates that NK-NVs exhibit a protein profile more similar to NK cells, whereas NK-EVs show significantly higher expression of granzyme B, a key cytotoxic protein. Western blot analysis further confirmed the relatively low expression of granzyme B in NK-NVs. Given the role of granzyme in NK cell-mediated target cell death, with rapid granule-mediated cell death which typically occurs within 24 hours, this could explain the slower cytotoxicity of NK-NVs on cancer cells compared to NK-EVs.[29,30] Additionally, the significantly higher expression of BiP, an endoplasmic reticulum (ER) chaperone, in NK-NVs may also contribute to this delayed effect. Previous studies have demonstrated that NK-EVs induce target cell death via ER stress.[25] The elevated BiP expression in NK-NVs suggests a potential link between BiP and their cytotoxicity, with ER stress likely playing a key role in the observed slower cytotoxicity.

Another key factor contributing to the slower cytotoxicity of NK-NVs may be the mechanism by which they enter cancer cells. Uptake experiments revealed that NK-NVs began accumulating in cancer cells at 3 hours, with significant uptake observed after 24 hours. Many studies have demonstrated that EVs are primarily internalized by cells via classical endocytosis mechanisms, the specific pathway depends on the surface proteins and glycoproteins present on both the vesicle and target cell.[31,32] In our study, pretreatment of cancer cells with MβCD significantly reduced the uptake of NK-NVs by cancer cells. Whereas MβCD is an inhibitor of caveolae-mediated endocytosis, which depletes cholesterol from the cell membrane, cholesterol is required for formation of caveolae.[33,34] This suggests that NK-NVs likely enter cancer cells through caveolae-mediated endocytosis pathway. Whereas, caveolae-mediated endocytosis is slower relative to clathrin-mediated endocytosis, which may also contribute to the slower uptake of NK-NVs by cancer cells.[35–37] Moreover, after pretreatment with MβCD, the cytotoxic effect of NK-NVS on cancer cells was inhibited, further demonstrating that cholesterol plays a crucial role in the internalization of NK-NVS by cancer cells. Since NK-NVs are formed by membrane disruption through shear or frictional forces, followed by rapid lipid bilayer reorganization, this process may alter NK-NVs membrane properties, including protein structures. Future research will explore whether this shear-based formation induces structural changes in the membrane, facilitating caveolae-mediated entry into cancer cells.

To evaluate the drug delivery capacity of NK-NVs, four different drug-loading strategies were tested for preparing NK-NVs-DOX. The goal was to identify the method that could balance maximum drug loading and recovery yield while maintaining minimal particle size. After considering drug loading efficiency, particle size, and recovery rate, extrusion emerged as the optimal preparation method. In this approach, a mixture of NK-NVs and DOX is passed through a lipid extruder with a porous membrane, efficiently loading the drug into the vesicles. This method demonstrated high drug loading efficiency, and the NK-NVs-DOX particles produced were uniform in size. Although both ultrasound and extrusion methods significantly killed cancer cells when applied to NK-NVs-DOX, the ultrasound method resulted in substantial loss, with a recovery rate only one-tenth that of extrusion. Therefore, extrusion is the optimal method for drug loading into NK-NVs.

The stability of the drug delivery carrier is an important factor influencing the efficacy of the drug delivery system. Our study demonstrated that the drug loading of NK-NVs-DOX remained stable at both 4°C and −80°C over a period of 28 days. This indicates that the stability of NK-NVs-DOX can be effectively maintained for at least 28 days at 4°C, greatly facilitating its subsequent application. In addition, compared to its release in a pH 5.5 solution, NK-NVs-DOX

released DOX more slowly in a pH 7.4 buffer. Given that the pH of normal blood is around 7.4, this suggests that NK-NVs-DOX remains stable in the bloodstream, allowing it to maintain a higher concentration of DOX before reaching the target tissue. Furthermore, NK-NVs-DOX exhibited a higher drug release rate at pH 5.5, which corresponds to the acidic tumor microenvironment. This facilitates the rapid release of DOX upon reaching the tumor, thereby increasing the effective drug concentration within the tumor tissue. Based on the in vitro result, the NK-NVs-DOX formulation will be administered intravenously via tail vein injection in tumor-bearing murine models for our planned in vivo studies.

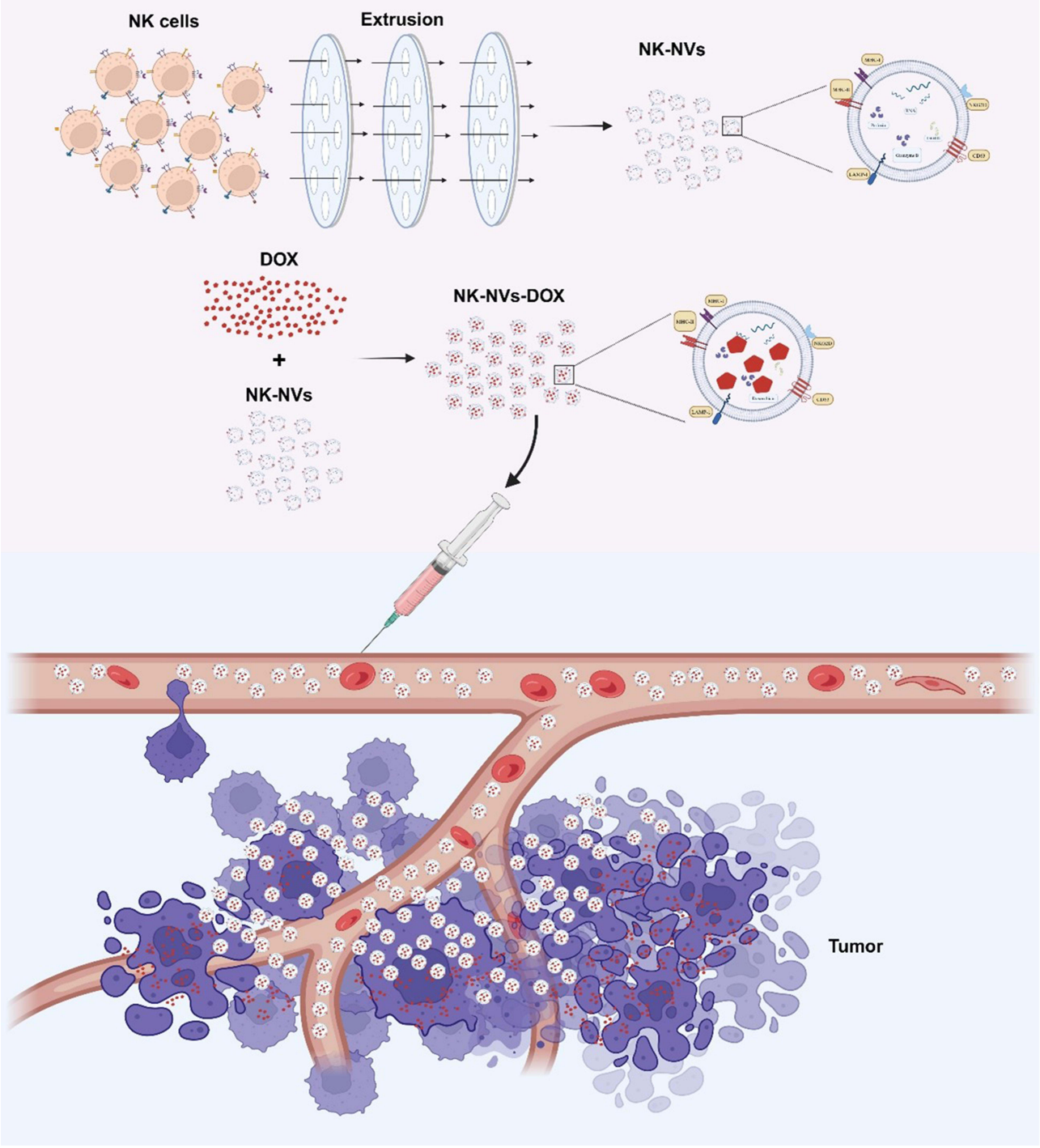

Figure 7 Schematic illustration of the generation process of NK- NVs and NK-NVs-DOX, and stability of NK-NVs-DOX during transportation in the bloodstream and its rapid release at the tumor site.

https://doi.org/10.2147/IJN.S527756

Subsequent investigations will focus on structural modifications of NK-NVs to enhance tumor-targeting capabilities through surface conjugation of tumor-specific ligands.

Conclusion

In summary, we systematically evaluated the potential application of NK-NVs prepared by extrusion method for antitumor therapy (Figure 7). Compared with the ultracentrifugation, the extrusion method can significantly increase the yield of NK-NVs, overcoming the challenge of large-scale production for clinical translation. NK-NVs prepared by extrusion exhibited similar cytotoxicity as NK-EVs, albeit at a relatively slower rate. This is likely due to differences in their internalization pathways by cancer cells. Additionally, the differential release of NK-NVs-DOX under pH 7.4 and pH 5.5 conditions ensures stability during blood transport and rapid released upon arrival at the tumor. This allows NK-NVs to be used as an efficient delivery vehicle for anti-cancer drug.

These findings demonstrate that NK-NVs can be used as a "cell-free" immunotherapeutic strategy, providing an alternative to cancer treatment. However, our study was limited to the cellular level, and the anti-cancer effects of NK-NVs in animals require further investigation. Nevertheless, our work may represent a starting point for further evaluation of the role of NK-NVs in tumor immunotherapy.

Acknowledgments

We extend our sincere gratitude to the Research Center for Basic Sciences of Medicine at Guizhou Medical University for providing the essential equipment and technical guidance that were instrumental in the successful completion of this project.

Author Contributions

All authors contributed to data analysis, drafting or revising the article, have agreed on the journal to which the article will be submitted, gave final approval of the version to be published, and agree to be accountable for all aspects of the work.

Funding

This work was supported by the National Natural Science Foundation of China (grant number: 82460604), Key Program for Science and Technology of Guizhou Province (grant number: ZK (2021)012) and Tumor Immunotherapy Technology Engineering Research Center (University Engineering Center, 2024 [001]) provided to Xing Zhao. Funded by the Guizhou Provincial Health Commission Science and Technology Fund Project (gzwkj2024-569) and Science and Technology of Guizhou Province (grant number: ZK [2024]115) provided to Jing Zhang. Funded by the Guizhou Provincial Health Commission Science and Technology Fund Project (gzwkj2022-087) provided to Liang Chen.

Disclosure

The authors declare that they have no known competing financial interests or personal relationships that could have appeared to influence the work reported in this paper.

References

1. Debbi L, Guo S, Safina D, et al. Boosting extracellular vesicle secretion. *Biotechnol Adv*. 2022;59:107983. doi:10.1016/j.biotechadv.2022.107983
2. Koh E-K, Lee H-R, Son W-C, et al. Combinatorial immunotherapy with gemcitabine and ex vivo-expanded NK cells induces anti-tumor effects in pancreatic cancer. *Sci Rep*. 2023;13(1):7656. doi:10.1038/s41598-023-34827-z
3. Myers JA, Miller JS. Exploring the NK cell platform for cancer immunotherapy. *Nat Rev Clin Oncol*. 2021;18(2):85–100. doi:10.1038/s41571-020-0426-7
4. Chulpanova DS, Kitaeva KV, James V, et al. Therapeutic prospects of extracellular vesicles in cancer treatment. *Front Immunol*. 2018;9:1534. doi:10.1038/s41423-024-01145-x
5. Takahashi Y, Takakura Y. Extracellular vesicle-based therapeutics: extracellular vesicles as therapeutic targets and agents. *Pharmacol Ther*. 2023;242:108352. doi:10.1016/j.pharmthera.2023.108352
6. Cieślik M, Bryniarski K, Nazimek K. Biodelivery of therapeutic extracellular vesicles: should mononuclear phagocytes always be feared?. *Front Cell Dev Biol*. 2023;11:1211833. doi:10.3389/fcell.2023.1211833

7. Wang L, Yu X, Zhou J, et al. Extracellular vesicles for drug delivery in cancer treatment. *Biol Proced Online*. 2023;25(1):28. doi:10.1186/s12575-023-00220-3
8. Luo H, Zhou Y, Zhang J, et al. NK cell-derived exosomes enhance the anti-tumor effects against ovarian cancer by delivering cisplatin and reactivating NK cell functions. *Front Immunol*. 2023;13:1087689. doi:10.3389/fimmu.2022.1087689
9. Wen Y, Fu Q, Soliwoda A, et al. Cell-derived nanovesicles prepared by membrane extrusion are good substitutes for natural extracellular vesicles. *Extracellular Vesicle*. 2022;1:100004. doi:10.1016/j.vesic.2022.100004
10. Ilahibaks NF, Lei ZY, Mol EA, et al. Biofabrication of cell-derived nanovesicles: a potential alternative to extracellular vesicles for regenerative medicine. *Cells*. 2019;8(12):1509. doi:10.3390/cells8121509
11. Lee H, Cha H, Park JH. Derivation of cell-engineered nanovesicles from human induced pluripotent stem cells and their protective effect on the senescence of dermal fibroblasts. *Int J Mol Sci*. 2020;21(1):343. doi:10.3390/ijms21010343
12. Wang L, Abhange KK, Wen Y, et al. Preparation of engineered extracellular vesicles derived from human umbilical cord mesenchymal stem cells with ultrasonication for skin rejuvenation. *ACS Omega*. 2019;4(27):22638–22645. doi:10.1021/acsomega.9b03561
13. Huang CC, Kang M, Lu Y, et al. Functionally engineered extracellular vesicles improve bone regeneration. *Acta Biomater*. 2020;109:182–194. doi:10.1016/j.actbio.2020.04.017
14. Wang X, Hu S, Zhu D, et al. Comparison of extruded cell nanovesicles and exosomes in their molecular cargos and regenerative potentials. *Nano Res*. 2023;16(5):7248–7259. doi:10.1007/s12274-023-5374-3
15. Zhu L, Gangadaran P, Kalimuthu S, et al. Novel alternatives to extracellular vesicle-based immunotherapy-exosome mimetics derived from natural killer cells. *Artif Cells Nanomed Biotechnol*. 2018;46(sup3):S166–S179. doi:10.1080/21691401.2018.1489824
16. Pan R, Ryan J, Pan D, et al. Augmenting NK cell-based immunotherapy by targeting mitochondrial apoptosis. *Cell*. 2022;185(9):1521–1538.e18. doi:10.1016/j.cell.2022.03.030
17. Chen X, Shi C, He M, et al. Endoplasmic reticulum stress: molecular mechanism and therapeutic targets. *Signal Transduct Target Ther*. 2023;8(1):352. doi:10.1038/s41392-023-01570-w
18. Di Pace AL, Tumino N, Besi F, et al. Characterization of human NK cell-derived exosomes: role of DNAM1 receptor in exosome-mediated cytotoxicity against tumor. *Cancers*. 2020;12(3):661. doi:10.3390/cancers12030661
19. Goh WJ, Lee CK, Zou S, et al. Doxorubicin-loaded cell-derived nanovesicles: an alternative targeted approach for anti-tumor therapy. *Int J Nanomed*. 2017;12:2759–2767. doi:10.2147/IJN.S131786
20. Tian J, Han Z, Song D, et al. Engineered exosome for drug delivery: recent development and clinical applications. *Int J Nanomed*. 2023;18:7923–7940. doi:10.2147/IJN.S444582
21. Page A, Chuvin N, Valladeau-Guilemond J, Depil S. Development of NK cell-based cancer immunotherapies through receptor engineering. *Cell Mol Immunol*. 2024;21(4):315–331. doi:10.1038/s41423-024-01145-x
22. Kaban K, Hinterleitner C, Zhou Y, et al. Therapeutic silencing of BCL-2 using NK cell-derived exosomes as a novel therapeutic approach in breast cancer. *Cancers*. 2021;13(10):2397. doi:10.3390/cancers13102397
23. Lou S, Hu W, Wei P, et al. Artificial nanovesicles derived from cells: a promising alternative to extracellular vesicles. *ACS Appl Mater Interfaces*. 2025;17(1):22–41. doi:10.1021/acsami.4c12567
24. Wu CH, Li J, Li L, et al. Extracellular vesicles derived from natural killer cells use multiple cytotoxic proteins and killing mechanisms to target cancer cells. *J Extracell Vesicles*. 2019;8(1):1588538. doi:10.1080/20013078.2019.1588538
25. Zhu Y, Huang B, Shi J. Fas ligand and lytic granule differentially control cytotoxic dynamics of natural killer cell against cancer target. *Oncotarget*. 2016;7(30):47163–47172. doi:10.18632/oncotarget.9980
26. Jarahian M, Marofi F, Maashi MS, et al. Re-expression of poly/oligo-sialylated adhesion molecules on the surface of tumor cells disrupts their interaction with immune-effector cells and contributes to pathophysiological immune escape. *Cancers*. 2021;13(20):5203. doi:10.3390/cancers13205203
27. Aldeghaither DS, Zahavi DJ, Murray JC, et al. A mechanism of resistance to antibody-targeted immune attack. *Cancer Immunol Res*. 2019;7(2):230–243. doi:10.1158/2326-6066.CIR-18-0266
28. Kim HA, Kim H, Nam M-K. Suppression of the antitumoral activity of natural killer cells under indirect coculture with cancer-associated fibroblasts in a pancreatic TIME-on-chip model. *Cancer Cell Int*. 2023;23(1):219. doi:10.1186/s12935-023-03064-9
29. Prager I, Liesche C, van Ooijen H, et al. NK cells switch from granzyme B to death receptor–mediated cytotoxicity during serial killing. *J Exp Med*. 2019;216(9):2113–2127. doi:10.1084/jem.20181454
30. Parolini I, Federici C, Raggi C, et al. Microenvironmental pH is a key factor for exosome traffic in cancer cells. *J Biol Chem*. 2009;284(49):34211–34222. doi:10.1074/jbc.M109.041152
31. Gandek T, van der Koog L, Nagelkerke AA, et al. Comparison of cellular uptake mechanisms, delivery efficacy, and intracellular fate between liposomes and extracellular vesicles. *Adv Healthc Mater*. 2023;12(25):2300319. doi:10.1002/adhm.202300319
32. Chen Y, Wang T, Yang Y, et al. Extracellular vesicles derived from PPRV-infected cells enhance signaling lymphocyte activation molecular (SLAM) receptor expression and facilitate virus infection. *PLoS Pathog*. 2022;18(9):e1010759. doi:10.1371/journal.ppat.1010759
33. Mulcahy LA, Pink RC, Carter DR. Routes and mechanisms of extracellular vesicle uptake. *J Extracell Vesicles*. 2014;3(1):24641. doi:10.3402/jev.v3.24641
34. Sandvig K, Torgersen ML, Raa HA, et al. Clathrin-independent endocytosis: from nonexisting to an extreme degree of complexity. *Histochem Cell Biol*. 2008;129(3):267–276. doi:10.1007/s00418-007-0376-5
35. Sahay G, Alakhova DY, Kabanov AV. Endocytosis of nanomedicines. *J Control Release*. 2010;145(3):182–195. doi:10.1016/j.jconrel.2010.01.036
36. Fang YP, Zhao YG, Sun CX, et al. Recent progress and future trends of food colloids: component interactions, future food structure design and colloidal nutrition. *Food Sci*. 2022;43(15):1–20. doi:10.7506/spkx1002-6630-20220510-123
37. Fu WY, Lei CH, Liu SW, et al. CAR exosomes derived from effector CAR-T cells have potent antitumour effects and low toxicity. *Nat Commun*. 2019;10(1):4355. doi:10.1038/s41467-019-12321-3